



HAL
open science

Spatiotemporal changes in the genetic diversity of harmful algal blooms caused by the toxic dinoflagellate *Alexandrium minutum*

Aliou Dia, Laure Guillou, Stéphane Mauger, Estelle Bigeard, Dominique Marie, Myriam Valero, Christophe Destombe

► To cite this version:

Aliou Dia, Laure Guillou, Stéphane Mauger, Estelle Bigeard, Dominique Marie, et al.. Spatiotemporal changes in the genetic diversity of harmful algal blooms caused by the toxic dinoflagellate *Alexandrium minutum*. *Molecular Ecology*, 2014, 23 (3), pp.549-560. 10.1111/mec.12617 . hal-01132961

HAL Id: hal-01132961

<https://hal.science/hal-01132961>

Submitted on 23 Mar 2015

HAL is a multi-disciplinary open access archive for the deposit and dissemination of scientific research documents, whether they are published or not. The documents may come from teaching and research institutions in France or abroad, or from public or private research centers.

L'archive ouverte pluridisciplinaire **HAL**, est destinée au dépôt et à la diffusion de documents scientifiques de niveau recherche, publiés ou non, émanant des établissements d'enseignement et de recherche français ou étrangers, des laboratoires publics ou privés.

SPATIOTEMPORAL CHANGES IN THE GENETIC DIVERSITY OF HARMFUL ALGAL BLOOMS CAUSED BY THE TOXIC DINOFLAGELLATE *ALEXANDRIUM MINUTUM*

A. Dia^{*}, L. Guillou, S. Mauger, E. Bigeard, D. Marie, M. Valero, C. Destombe^{*}

UPMC Paris VI, UMR 7144, Adaptation et diversité en milieu marin, Station Biologique de Roscoff, Place Georges Teissier, CS 90074, 29688 Roscoff, France.

CNRS, UMR 7144, Adaptation et diversité en milieu marin, Station Biologique de Roscoff, Place Georges Teissier, CS 90074, 29688 Roscoff, France.

Keywords: population genetics, bloom dynamics, resting cyst, linkage disequilibrium, sexual reproduction, clonality.

***Corresponding authors:** Aliou Dia, Christophe Destombe

Address: Station Biologique de Roscoff, Place Georges Teissier, CS 90074, 29688 Roscoff, France.

Emails: adia@sb-roscoff.fr, destombe@sb-roscoff.fr

Running title: *A. minutum* spatiotemporal genetic diversity

Word count: 6968

Table count: 4

Figure count: 2

Supporting information: Dia_etal_suppinfo.doc; contains datasets.

Abstract

Organisms with sexual and asexual reproductive systems benefit from both types of reproduction. Sexual recombination generates new combinations of alleles whereas clonality favors the spread of the fittest genotype through the entire population. Therefore, the rate of sexual versus clonal reproduction has a major influence on the demography and genetic structure of natural populations. We addressed the effect of reproductive system on populations of the dinoflagellate *A. minutum*. More specifically, we monitored the spatiotemporal genetic diversity during and between bloom events in two estuaries separated by 150 km for two consecutive years. An analysis of population genetic patterns using microsatellite markers revealed surprisingly high genotypic and genetic diversity. Moreover, there was significant spatial and temporal genetic differentiation during and between bloom events. Our results demonstrate that (1) interannual genetic differentiation can be very high, (2) estuaries are partially isolated during bloom events, and (3) genetic diversity can change rapidly during a bloom event. This rapid genetic change may reflect selective effects that are nevertheless not strong enough to reduce allelic diversity. Thus, sexual reproduction and/or migration may regularly erase any genetic structure produced within estuaries during a bloom event.

Introduction

The demography and genetics of natural populations can vary according to the rate of sexual versus clonal reproduction. These two modes of reproduction occur simultaneously in many eukaryotes. These species can benefit both from the advantage of sexual reproduction, which lies in the genetic recombination that it generates, and from the theoretical short-term demographic advantage of clonal reproduction (Maynard-Smith 1978). The relative contribution of sexual and asexual reproduction can vary within a species depending on environmental conditions (Eckert 2001; Silvertown 2008). For example in aphids, sexual reproduction is associated with the production of resting eggs that can survive harsh conditions, whereas populations living in milder environments may reproduce asexually throughout the whole year (Rispe *et al.* 1998). Sexual reproduction thus seems required to produce a resistant form, regardless of the genetic variability generated. In the freshwater microcrustacean *Daphnia pulex* that practices facultative sexual reproduction (alternation between parthenogenesis and sexual reproduction) during the growing season, selection on clonal lines results in an increase in genotypic adaptation and an erosion in clonal diversity (Deng & Lynch 1996). The over-representation of certain clonal genotypes at the end of the growing season leads to greater genetic structuring and linkage disequilibrium. Similarly, most plankton species alternate between an active growing phase, during which the number of cells increases rapidly, and another phase, generally involving sexual reproduction, during which cells are in a dormant state. During the asexual reproduction phase, fitness differences among clonal lineages may cause rapid changes in genotype frequencies. In the cyclically parthenogenetic rotifer species *Brachionus plicatilis*, there is evidence that clonal selection occurs during the parthenogenetic phase (Gómez & Carvalho 2000). However, sexual reproduction as well as dormant stages may slow down the response to directional selection

and may act to maintain genetic variation when selection fluctuates (Hairston *et al.* 1996). Thus, in the freshwater copepod *Diaptomus sanguineus*, the dormant cells may act as a reservoir of genotypes (similar to a seed bank) produced in past environments, but they also may interact as a part of the selection-response dynamics in the current environment (Hairston *et al.* 1996).

An extreme case of alternation of an asexual growing phase and a dormant sexual phase is exemplified by unicellular phytoplankton bloom species involved in harmful algal blooms (HABs). Compared to multicellular organisms, these unicellular organisms are characterized by a ubiquitous distribution, suggesting very large population sizes and broad dispersal abilities (Cloern 1991; Finlay & Fenchel 2004; Norris 2000). Nevertheless, dispersal of marine phytoplankton is a hotly debated issue and published results are subject to controversies. Studies on marine phytoplankton dispersal differ vastly with respect to study scale, sampling strategy (e.g. sampling few individuals per global geographic region; population samples) and the resolution of the characters or markers used (e.g. morphological markers; highly variable, microsatellite-type molecular markers). For example, using morphological criteria, Cermeno and Falkowski (2009) argue that the biogeographical distribution of fossil diatom genera is ubiquitous and that these taxa thus have no geographic structure. However, more recent studies using microsatellite markers demonstrate that there is genetic differentiation within a single species, the toxic diatom *Pseudo-nitzschia pungens*, on a very large scale (i.e. samples from the Atlantic and Pacific Oceans) (Casteleyn *et al.* 2010). The issue of connectivity between populations remains unresolved because there is little information on the distance that a single phytoplankton cell can cover and because there are only a few studies on how the marine physical environment influences dispersal. Exploring these factors is necessary for a better understanding of the ecology and evolution of plankton

organisms (Palumbi 1994). Over the past several years, more and more studies have focused on spatiotemporal differentiation in dinoflagellate populations. For example, in the Gulf of Maine, genetic differentiation was found between two subpopulations investigated during offshore blooms, corresponding to the beginning and the end of a bloom event (which lasts about 2 months), but in different geographic locations (northern and southern, separated by hundreds of km) (Erdner *et al.* 2011). Other work (Richlen *et al.* 2012) shows spatiotemporal differentiation in the estuaries of Massachusetts (Nauset Marsh system and the Gulf of Maine) at two sites, but only one site was sampled throughout the whole bloom event (from beginning to end), precluding any comparison between dates of the same bloom at different sites. Whatever their scale, these previous studies demonstrate genetic differentiation between sites and high genetic diversity within a given bloom event. This differentiation of bloom populations and their high genetic diversity leads to questions on the role of the two life-cycle phases on population dynamics and the importance of sexual reproduction relative to clonal reproduction.

The dinoflagellate *Alexandrium minutum* (Halim 1960) is one of the main species involved in paralytic shellfish poisoning (PSP) blooms off the coasts of France. This microalga produces saxitoxins that can accumulate along the trophic food web. They produce PSP events that cause cases of human poisoning, typically by ingestion of contaminated shellfish. This species shows an alternation of asexual and sexual phases. The vegetative cell is haploid and sexual reproduction takes place when the environmental conditions become unfavorable (Figueroa *et al.* 2011). Sexual reproduction is the result of the fusion between two gametes, forming a planozygote (Probert *et al.* 2002). This stage changes into a resting cyst that sinks to the sediment (like seeds in a seed bank) (Wyatt & Jenkinson 1997). After a dormancy period of several months (Garcés *et al.* 2004; Figueroa *et al.* 2007), cysts may

germinate and give rise to vegetative haploid cells that reproduce asexually in the water column.

The objective of this study was to study the effect of asexual and sexual reproduction on the population genetic structure of this toxic dinoflagellate *A. minutum* on a small scale, both in space and in time. We used microsatellite markers to analyze monoclonal cultures of *A. minutum* isolated from samples taken at two sites located along the French coast of the English Channel, separated by roughly 150 km, for two consecutive annual bloom events and at three different periods during each bloom event. We specifically addressed the following questions: (1) To what degree are different estuaries within the same geographic region connected? (2) What role does sexual reproduction play in the dynamics of the bloom populations? (3) Finally, is there any temporal genetic structuring during bloom events?

Materials and Methods

Sampling sites and strain collection

More than 1240 strains of dinoflagellates (different species) were collected in the Penzé estuary (48°37'37.57"N, 3°57'13.17"W) and the Rance estuary (48°31'49.61"N, 1°58'21.81"W, Table 1). These two estuaries are separated by approximately 150 km (Fig. 1). *A. minutum* blooms occurred concomitantly in both ecosystems in early summer. In 2010, blooms extend from 17 May to 12 July in the Rance estuary (maximum density of 4.2×10^4 cells/L⁻¹ observed on June 22) and from 2 June to 7 July in the Penzé estuary (maximum density of 3.7×10^5 cells/L⁻¹ observed on 8 June). In 2011, blooms lasted from 11 May to 20 June in Rance (maximum density of 4.3×10^5 cells/L⁻¹ observed on 27 May) and from 1 June to 8 July in Penzé (maximum density of 2.6×10^5 cells/L⁻¹ observed on 23 June).

Plankton samples were collected from these two sites during the developmental phase of the bloom (beginning), during the maintenance phase (middle) and during the decline phase (end of the bloom event) whenever possible in each of two study years (2010 and 2011). All strains were obtained by micropipetting one single cell into fresh medium; 530 of these strains survived and 265 strains of *A. minutum* were genotyped. They were maintained at 19°C with 70 $\mu\text{E}\cdot\text{m}^2\cdot\text{s}^{-1}$ of light in a 12:12 light:dark cycle. The medium F/2 (Marine Water Enrichment Solution, Sigma) was prepared using autoclaved natural seawater from the Penzé estuary. It was collected at least 3 months prior to use and stored in the dark. Strains used in this study (see supplementary Table S1) have been deposited at the Roscoff Culture Collection (www.sb-roscoff.fr/Phyto/RCC).

Flow cytometry

The DNA content of each monoclonal strain was checked by flow cytometry on whole *A. minutum* cells fixed in ethanol. A 250 μL aliquot of each culture was centrifuged at 3000 rpm for 10 min. The supernatant was removed, cells were then re-suspended by vortexing in 250 μL of 70% ethanol and kept overnight at 4°C. Cells were collected by centrifugation at 3000 rpm for 10 min to remove ethanol and then resuspended in 250 μL of PBS. Triton X-100 (0.1% final), RNase A (0.01%) and Propidium Iodide (PI, 30 $\mu\text{g}\cdot\text{mL}^{-1}$) were added. Samples were incubated at 37°C for 30 min before flow cytometry analysis, performed using a FACS Canto II (Becton Dickinson, San Jose, CA, USA) flow cytometer equipped with a 488 nm laser and the standard filter setup. The DNA content of *A. minutum* strains was evaluated by comparison with Human Blood Cells (HBCs, 2C = 6.4 Mbp). Isolated nuclei of human blood cells were obtained by resuspending 10 μL of blood in 1 mL of NIB buffer (Marie *et al.* 2000). Then, 10 μL of this suspension was added to 250 μL of *A. minutum* culture re-suspended in PBS buffer before staining. Then, all cultures were analyzed by flow

cytometry without HBC and mean fluorescence of PI were compared to check for ploidy level differences.

DNA extraction, strain identification and genotyping

For DNA extraction, strains were collected during their exponential growth stage (strains listed Table 1). DNA was extracted using either the CTAB method (Lebret *et al.* 2012) or the Nucleospin 96 Plant kit (Macherey-Nagel, Düren, Germany), according to the manufacturer's instructions, using 5-10 mg of dried tissue resuspended in 100 µL elution buffer.

Strains were screened using the intergenic region of ribosomal DNA (ITS1, 5.8S and ITS2). PCR mixes (14 µL in total) included 20 ng of DNA, 1X GoTaq Flexi green buffer (Promega, Madison, WI, USA), 150 µM of each dNTP (Thermo Fisher Scientific Inc., Waltham, MA, USA), 20 pmol of the forward primer 329F (5'-GTG AAC CTG CRG AAG GAT CA-3', complementary reverse of the eukaryote reverse primer 329-R (Moon-van der Staay *et al.* 2001), 20 pmol of the reverse primer DIR-R (5'- TAT GCT TAA AAT TCA GCA GGT-3' (Scholin & Anderson 1994), and 1.25 U GoTaq® Polymerase (Promega). Amplification was carried out in a DNA Engine Peltier Thermal Cycler (Bio-Rad, Hercules, CA, USA) with the following cycling conditions: an initial denaturation at 95°C for 5 min, followed by 35 PCR cycles (denaturation at 95°C for 45 s, annealing at 53°C for 45 s, and extension at 72°C for 45 s), followed by a final extension at 72°C for 10 min. The PCR products were purified using the BigDye® Terminator v3.1 Cycle Sequencing kit (Applied Biosystems, Foster City, CA, USA) for subsequent bidirectional sequencing using a capillary sequencer type ABI 3130XL (Applied Biosystems).

The strains were genotyped using the 12 microsatellite markers developed by (Nagai *et al.* 2006). Amplification of microsatellite loci was carried out in a 10 µL final volume with the

following components: 20 ng DNA, 1x GoTaq® Flexi buffer (Promega), 2 mM MgCl₂, 150 μM each dNTP (Thermo Fisher Scientific Inc.), 0.8 μg.μL⁻¹ bovine serum albumin, 30 pmol fluorescent-labeled forward primer (FAM, VIC, NED or PET), 30 pmol reverse primer, and 0.35 U GoTaq® Polymerase (Promega). PCR amplifications were carried out in a Bio-Rad DNA Engine Peltier Thermal Cycler using the following cycling conditions: an initial denaturation at 95°C for 5 min, followed by 10 PCR cycles (denaturation at 95°C for 30 s, annealing at 60°C for 30 s and extension at 72°C for 30 s) followed by 28 cycles (denaturation at 95°C for 30 s, annealing at 55°C for 30 s and extension at 72°C for 30 s), followed by a final extension at 72°C for 10 min. Then, 2 μL of PCR products, diluted 1:10, was added to 10 μL of loading buffer containing 0.5 μL of SM594 size standard (Mauger *et al.* 2012) and 9.5 μL of Hi-Di formamide (Applied Biosystems). The loading mix was denatured at 95°C for 3 min and run in an ABI 3130 XL capillary sequencer (Applied Biosystems) equipped with 50 cm capillaries. Genotypes were scored manually using GeneMapper version 4.0 (Applied Biosystems).

Genetic analyses

To increase sample size, close sampling dates were pooled (i.e. PZ10D, PZ11B and RC11D, Table 1) and ultimately only 11 samples with a minimum sample size of 15 strains were used in the genetic analysis (i.e. RC10D was excluded from the analyses; see Table 1).

Genetic diversity and multilocus genotype diversity

Because strains of *A. minutum* are haploid, the frequencies of null alleles were estimated by direct observation. After two re-amplifications, strains for which more than half of the loci did not amplify correctly were removed from the dataset. The absence of amplification at loci in other strains was considered as a null allele. Standard measures of genetic diversity (mean

number of alleles per locus (N_a), Nei's unbiased estimator of genetic diversity (H_s ; Nei 1987), and allelic richness (R_a) for each sampling date and site were calculated using Fstat (version 2.9.3.2; Goudet 2001). Allelic richness was estimated after randomly subsampling each sample (10,000 randomizations) to standardize the minimum sample size among populations. Test for differences among groups, Fstat (Goudet 2001) was used to test the difference between the H_s values obtained at the beginning phases (PZ11A, RC10A, RC11A) and at the end phases of bloom events (PZ10D, PZ11D, RC11D). Genclone (Arnaud-Haond *et al.* 2005) was used to test the efficiency of the microsatellite marker set to discriminate the maximum clonal diversity available in the data set and to calculate the number of distinct multilocus genotypes observed (G).

Linkage Disequilibrium

Linkage disequilibrium (LD) was assessed using a single multilocus measurement of LD that is provided by the association index \bar{r}_d (Brown *et al.* 1980 modified by Agapow & Burt 2001) and was computed using MultiLocus ver 1.2. (Agapow & Burt 2001). Significance tests were based on comparisons of the observed value to those of randomized datasets generated from 1000 permutations (Burt *et al.* 1996). The global P -value was calculated using a generalized binomial procedure to combine independent data (Teriokhin *et al.*, 2007; De Meeûs *et al.*, 2009).

Genetic differentiation

F_{st} values were calculated between all pairs of populations using GENETIX 4.05 (Belkhir *et al.*, 1996-2004), their significance was assessed using 1.000 permutations and D (D_{est} ; Jost, 2008) was estimated with SMOGD 1.25 (Crawford, 2010). Different levels of comparison were thus considered: among dates during a bloom event, among dates within a

site, and between sites. These data were summarized and statistically tested with a principal component analysis (PCA) performed using PCA-GEN software (version 1.2; Goudet 1999). The statistical significance associated with each axis was evaluated after 10,000 randomizations.

The partitioning of genetic variation at different hierarchical levels was examined using molecular analyses of variance (AMOVA) in Arlequin 3.5.1.2 (Excoffier & Lischer 2010). There was only one sampling date during the 2010 bloom in Rance (Table 1); it was therefore only possible to conduct the two following analyses. First, variation was assessed on the 2011 samples by determining the variance component attributable to between-sites differentiation and to among in-bloom phases within a site. Second, variation was examined in more detail only at Penzé by determining the variance component attributable to between-years differentiation and to among in-bloom phases within years. The significance ($P < 0.05$) of the fixation indices was evaluated based on 10,000 permutations.

Results

Isolation and identification of strains

Of the 1240 isolated cells, we obtained 530 usable strains for this study (i.e. 43% success rate). The survival rate by sampling date ranged from 27% to 66%. Of these 530 monoclonal strains, 364 (66%) were assigned to *A. minutum* showing a unique haplotype corresponding to 100% similarity with a 550 bp of the rDNA sequence (covering ITS1, the 5.8S rRNA gene, and ITS2) (McCauley *et al.* 2009; Casabianca *et al.* 2011) were selected (Table 1). Indeed, this unique sequence corresponds to an *A. minutum* sequence (AM1 strain) previously published in GenBank (EU707466). The comparison of *A. minutum* DNA content

shows that whole cells of *A. minutum* analyzed contain the same level of ploidy (32 Mbp, Fig. S1).

Genetic diversity

After re-amplifying strains with dubious amplification, 5 of the 12 loci (Aminu39, Aminu44, Aminu10, Aminu15 and Aminu29) developed by Nagai *et al.* (2006) were removed from the dataset. We also removed strains for which more than half of the loci did not amplify correctly. The final dataset included seven loci amplified on 265 individual strains (Table S2). For these loci, the frequency of null alleles varied from 8% for locus Aminu11 to 22% for locus Aminu20. The efficiency of the microsatellite loci to discriminate the maximum clonal diversity available in the sample is given Fig. S2. Of the 265 strains analyzed, 265 (100%) had unique seven-locus genotypes; there were therefore no repeated genotypes in any of the analyzed strains.

The PCR products of these seven microsatellite markers showed one single band, i.e. one allele. All loci were polymorphic. The genetic diversity indices are given in Table 2. The number of alleles varied among bloom populations, with some populations having twice as many alleles as other populations (cf. RC11A and RC10A, Table 2), and with sampling effort. Allele richness, corrected for sampling size, varied from 6.49 (RC11A) to 9.01 (RC11C). The per-locus and per-population numbers of alleles (N_a) ranged from 3 (locus A41) to 17 (locus A20) alleles. Whatever the sampling date during bloom events, Penzé and Rance showed high genetic diversities, with H_s values ranging from 0.79 to 0.88. These genetic diversity values did not differ between the beginning and the end phases of a bloom event within an estuary (permutation test of comparison among groups; P -value=0.647).

Tests of linkage disequilibrium revealed an overall P -value of 0.525. Of the 11 spatio-temporal samples, only one showed significant \bar{r}_d (i.e. linkage disequilibrium estimator)

values. This sample from Penzé (PZ11D) had a P -value of 0.047, with \bar{r}_d values of 0.068 (Table 3).

Genetic differentiation

The results of the PCA (Fig. 2) show a significant overall F_{st} value of 0.073. The first two PCA axes were significant and explained 44% of the variance: axis 1 accounts for 26.39% of the variance ($F_{st}= 0.019$, $P=0.001$) and axis 2 accounts for 17.65% of the variance ($F_{st}=0.013$, $P=0.011$). Axis 1 separates samples from the beginning of the 2010 bloom (PZ10A-RC10A) from the rest of the samples (Fig. 2). Axis 2 separates samples according to the sampling date during a bloom and their geographic origin. Samples from the beginning of the bloom were less genetically differentiated than samples from the end of the bloom events. These last samples formed distinct clusters according to their geographic origin (Fig. 2; cf. PZ11C, PZ11D compared to RC11D and RC11C).

Genetic differentiation between pairs of samples (F_{st}) ranged from -0.0035 (RC11A vs. RC11B) to 0.0770 (RC10A vs. PZ11C), whereas D_{est} ranged from 0.0589 (RC11B vs. RC11C) to 0.4695 (RC10A vs. PZ11C) (Table 3S). The lowest F_{st} values were observed for two samples from the same site in the same year at two consecutive in-bloom sampling dates, whereas the highest values were observed for samples between different sites and different years. The tests of differentiation at different spatial and temporal levels confirm the PCA results. They indicate that the early bloom samples in Penzé and Rance taken in 2010 (PZ10A and RC10A) differed significantly from all other samples (Table S3).

The first AMOVA helped gauge the importance of spatial variation with respect to phase variation within a bloom. This AMOVA could only be applied on the 2011 samples (Table 4A) and revealed that the genetic differentiation was significant between sites and among bloom phases within sites. More specifically, the percent of variation explained by the

genetic differentiation during the different phases of the bloom event was three times higher (3.87%) than the genetic differentiation between the Penzé and Rance sites (1.23%, Table 4A).

The second AMOVA was used to analyze the importance of temporal variation at two hierarchical levels: interannual and intrabloom (Table 4B). This temporal AMOVA could only be applied to the Penzé estuary. The results show again that the two levels of differentiation were significant. The percent variation explained by genetic differentiation between the different in-bloom periods was weaker (4.27%, Table 4B) than that explained by genetic differentiation between 2010 and 2011 (10.01%, Table 4B).

Discussion

Clonal reproduction versus sexual reproduction

The reproductive system can play an important role in the functioning and evolution of populations by modifying their dynamics, their diversity and their population genetic structure. As in many other phytoplankton species, the dinoflagellate species *A. minutum* is characterized by high rates of clonal reproduction during the development of bloom events, followed by a period of sexual reproduction that produces resting cysts, coinciding with the maximum and the decline of cell concentrations, respectively (Garcés *et al.* 2004, Bravo *et al.* 2010). During periods of asexual division, differences in selective values between clonal lines can rapidly lead to differences in genotype frequencies. Numerical simulations show that selective sweeps can occur when rapidly growing clones become more abundant within a population (Rynearson & Armbrust 2000). During a bloom event, advantageous genotypes may increase in frequency, leading to an overall decrease in genetic diversity via genetic hitchhiking over the whole genome (Maynard-Smith *et al.* 1993). Even in the absence of

selection, low clonal diversity and linkage equilibrium provide evidence that sexual reproduction occurs in a population with clonal reproduction. At the end of a bloom, the most frequent clones would thus preferentially participate in the production of the following generation via sexual reproduction. However, in rapidly growing organisms with short generation times, the huge population sizes can be considered as virtually infinite and genotypic diversity can thus be maintained during the bloom events, even if organisms primarily reproduce clonally (Bengtsson 2003).

In this study, all the analyzed clones were genetically distinct, suggesting that bloom events involve huge effective population sizes. The high genetic diversity observed here indicates that asexual reproduction does not predominate within *A. minutum* populations. It however does suggest that blooms were initiated by numerous different sexual cysts. Our results corroborate the recent observations reported for *Alexandrium fundyense* showing unique multilocus genotypic frequencies of 81% to 97% (Erdner *et al.* 2011; Richlen *et al.* 2012). Likewise, a study on *Alexandrium tamarense* has shown that the probability of sampling clones with the same genotype is practically nil due to the large population sizes of blooms (Nagai *et al.* 2007). The high genotypic diversity as well as the high gene diversity values observed in our study ($0.78 < H_s < 0.87$) are comparable to those of Mediterranean populations of the same species ($0.62 < H_s < 0.89$; Casabianca *et al.* 2011). There are reports of similar high genotypic diversity values in other phytoplankton species, such as the haptophyte (*Prymnesium parvum*) and the Raphidophyceae species (*Gonyostomum semen*) using AFLP genetic markers (Barreto *et al.* 2011; Lebret *et al.* 2012).

The continuous germination of resting cysts during the entire bloom event (Lebret *et al.* 2012), as well as the specific cohort of these cysts produced during successive annual blooms and stored in the cyst bank, may enhance genetic diversity (in terms of genotypes and genes)

(Alpermann *et al.* 2009). Furthermore, we cannot exclude the possibility that sexual reproduction maintains genetic diversity, even during a bloom event. Observations in *in vitro* cultures suggest that the zygote (planozygote) may undergo meiosis without forming a resting cyst (Figueroa *et al.* 2007), thereby producing new vegetative cells. This type of reproduction may be promoted by the presence of the parasite *Parvilucifera sinerae* (Alveolata), and short-circuiting the resting cyst stage may possibly constitute a strategy to avoid the parasite (Figueroa *et al.* 2010). Two different species belonging to genus *Parvilucifera* were detected during the 2010 and 2011 sampling cruises (Lepelletier *et al.* submitted). However, unfortunately, there have been no investigations to identify this type of reproduction.

In our study, no global multilocus linkage disequilibrium was detected, suggesting that recombination is sufficient to break down linkages between loci, confirming that *A. minutum* reproduces sexually. Only one sample taken during the late bloom period in Penzé in 2011 (PZ11D) showed significant multilocus linkage disequilibrium, as estimated using \bar{r}_d .

Spatiotemporal genetic structure of bloom events

The results of the microsatellite analysis clearly indicate that *A. minutum* blooms are structured both in space and in time. Our study shows that there is a temporal genetic differentiation during and between *A. minutum* blooms as well as spatial differentiation between sites. Thus, the overall genetic differentiation observed between the Rance and Penzé estuaries separated by roughly 150 km was significant. This result suggests that gene flow via tidal currents is limited in *A. minutum*, as demonstrated in *A. tamarense* (Nagai *et al.* 2007). Given the short duration of *A. minutum* bloom events (30 days on average) and that they are geographically restricted to estuaries, the gene flow between populations is likely limited. Genetic differences observed between the two estuaries late bloom samples confirm the genetic isolation between estuaries during the bloom period. However, early bloom samples

showed weaker spatial differentiation (Table 4). This observation suggests that the Penzé and Rance estuaries communicate during spring tides, potentially transporting vegetative cells or cysts via the residual west-east tidal currents. During the bloom season, which preferentially occurs during neap tides, the two estuaries are likely isolated and the accumulation of bloom biomass is mainly due to a response to water flow and to constant, suitable environmental conditions (i.e. salinity temperature, irradiance and nutrient supply) (Anderson *et al.* 2012). In our study, interannual genetic differentiation was greater than intrabloom differentiation, suggesting that blooms are not only made up of newly formed cysts produced during the preceding year, but also of recruitment from migrant vegetative cells and/or from an older cyst bank (Estrada *et al.* 2010). Even if a multigenerational cyst bank gives rise to a bloom event, the germination of cysts may be influenced by environment conditions and, by chance or selection, samples become more differentiated than the more homogeneous cyst bank that produced them (McCue & Holtsford 1998). The constant germination of the cyst bank may thus lead to a decrease in the interannual F_{st} . Nevertheless, the cyst bank does not appear to contribute regularly to bloom events because the 2010 Penzé sample PZ10D was not genetically different from the early 2011 Penzé bloom sample (PZ11A). Therefore, the 2011 early bloom sample may have been composed at least partly of cysts produced in the preceding year.

In isolated estuaries, there were significant genetic changes during a bloom event (see AMOVA, Table 4A). Although no additional signatures of selection, such as multilocus linkage disequilibrium, could be detected with the neutral markers used in this study, we believe that, in these very large populations, genetic changes may nevertheless be driven by selection (see below). These genetic changes are concordant with those reported for *A. fundyense* blooms in Massachusetts where temporal intrabloom differentiation has also been

observed (Richlen *et al.* 2012). Two factors can account for this temporal differentiation. First, changes may be due to delayed germination of different cohorts of cysts buried in the sediments and/or continuous encystment by a small percentage of motile cells (Pitcher *et al.* 2007). In *Gonyostomum semen* (Raphidophyceae), Lebret *et al.* (2012) suggest that continuous germination of cysts during a bloom is a key element behind rapid genetic changes. Second, these changes may be the result of local abiotic or biotic selection as suggested for the diatom *Ditylum brightwellii* (Rynearson & Armbrust 2005; Rynearson *et al.* 2006). In these large populations, the effects of natural selection may predominate over those of genetic drift on genetic structure. Thus, in *D. brightwellii*, the succession of genetically distinct populations in different environmental conditions appears to reflect a tight coupling between environment and genetics (Rynearson *et al.* 2006). Of the various abiotic factors, seasonal temperature variation is one parameter that can explain the maintenance of genetic diversity (Maynard-Smith and Hoekstra 1980; Bell 1982). Recent studies on the diatom *Asterionella formosa* have demonstrated that variation in temperature may contribute to maintaining genetic diversity in blooms (Gsell *et al.* 2012). In this species, reaction norms of clone growth studied as a function of environmental temperature reveal considerable genetic diversity within a bloom. In our study, fluctuating temperatures may explain not only the maintenance of genetic diversity, but also genetic changes during a bloom event. However, biotic factors, such as predation and/or parasitism, may also play a role in determining population structure and dynamics (Montagnes *et al.* 2008). In *A. minutum*, eukaryotic parasites such as *Parvilucifera* spp. and *Amoebophrya* spp. can regulate blooms (Chambouvet *et al.* 2008; Figueroa *et al.* 2010; Lepelletier *et al.* submitted). The impact of parasitism can be tested by analyzing the fitness of different strains and their resistance to parasites according to date and sampling site. Whatever the factors involved, our study illustrates how sexual

reproduction and/or migration are likely to erase any selective effects that arise each year during the vegetative phase of a bloom event.

Acknowledgements

We are very grateful to Yannis Michalakis, Denis Roze and Carolyn Engel for constructive comments on an earlier draft and 3 anonymous reviewers who helped improve this manuscript. We warmly thank the IFREMER laboratory in Dinard (France) and especially Claude Lebec and Claire Rollet. Thanks to the Roscoff Culture Collection (RCC), Service Mer et Observation (Marine Operations Department) at the Roscoff Biological Station and all the partners in the Paralex project for their help with sampling. Sequences and microsatellite genotypes were generated by Morgan Perennou and Gwenn Tanguy at the Roscoff Biological Station (Ouest-Géopole). This project was carried out in partial fulfillment of Aliou Dia's PhD degree, supported by funds from the ANR and a PhD fellowship from the Brittany Regional Council (ARE10087: POPALEX). This work was financially supported by the Brittany Regional Council, the CNRS program EC2CO, the French ANR projects PARALEX ("The sixth extinction" ANR-2009-PEXT-01201) and CLONIX ("Programme Blanc" ANR11-BSV7-00704), the European Project MaCuMBa (FP7-KBBE-2012-6-311975) and the EC2CO project PALMITO.

References

- Agapow P-M, Burt A (2001) Indices of multilocus linkage disequilibrium. *Molecular Ecology Notes*, **1**, 101-102.
- Alpermann TJ, Beszteri B, John U, Tillmann U, Cembella AD (2009) Implications of life-history transitions on the population genetic structure of the toxigenic marine dinoflagellate *Alexandrium tamarense*. *Molecular Ecology*, **18**, 2122-2133.
- Anderson, D M, Alpermann, T J, Cembella, A D, Collos, Y, Masseret, E, Montresor, M (2012). The globally distributed genus *Alexandrium*: Multifaceted roles in marine ecosystems and impacts on human health. *Harmful Algae*, **14**, 10-35.
- Arnaud-Haond S, Belkhir K (2007) GenClone 1.0: a new program to analyse genetics data on clonal organisms. *Molecular Ecology Notes*, **7**, 15–17.
- Barreto FS, Tomas CR, McCartney MA (2011) AFLP fingerprinting shows that a single *Prymnesium parvum* harmful algal bloom consists of multiple clones. *Journal of Heredity*, **102**, 747-752.
- Belkhir K, Borsa P, Chikhi L, Raufaste N Bonhomme F (1996-2004) *GENETIX 4.05, logiciel sous Windows TM pour la génétique des populations*. Laboratoire Génome, Populations, Interactions, CNRS UMR 5171, Université de Montpellier II, Montpellier, France.
- Bell G (1982) *The masterpiece of nature: the evolution and genetics of sexuality* Springer.
- Bengtsson BO (2003) Genetic variation in organisms with sexual and asexual reproduction. *Journal of evolutionary biology*, **16**, 189-199.
- Bravo I, Isabel Figueroa R, Garcès E, Fraga S, Massanet A (2010) The intricacies of dinoflagellate pellicle cysts: The example of *Alexandrium minutum* cysts from a bloom-recurrent area (Bay of Baiona, NW Spain). *Deep Sea Research Part II: Topical Studies in Oceanography*, **57**, 166-174.

- Brown AH, Feldman MW, Nevo E (1980) Multilocus structure of natural populations of *Hordeum spontaneum*. *Genetics*, **96**, 523-536.
- Burt A, Carter DA, Koenig GL (1996) Molecular markers reveal cryptic sex in the human pathogen *Coccidioides immitis*. *Proceedings of the National Academy of Sciences. USA*, **93**, 770-773
- Casabianca S, Penna A, Pecchioli E, et al. (2011) Population genetic structure and connectivity of the harmful dinoflagellate *Alexandrium minutum* in the Mediterranean Sea. *Proceedings of the Royal Society B: Biological Sciences*, **279**, 129-138.
- Casteleyn G, Leliaert F, Backeljau T, et al. (2010) Limits to gene flow in a cosmopolitan marine planktonic diatom. *Proceedings of the National Academy of Sciences*, **107**, 12952-12957.
- Cermeno P, Falkowski PG (2009) Controls on diatom biogeography in the ocean. *Science*, **325**, 1539-1541.
- Chambouvet A, Morin P, Marie D, Guillou L (2008) Control of toxic marine dinoflagellate blooms by serial parasitic killers. *Science*, **322**, 1254-1257.
- Cloern JE (1991) Tidal stirring and phytoplankton bloom dynamics in an estuary. *Journal of marine research*, **49**, 203-221.
- Crawford NG (2010) SMOGD: software for the measurement of genetic diversity. *Molecular Ecology Resources*, **10**, 556-557.
- De Meeûs T, Guégan JF, Teriokhin AT (2009) MultiTest V.1.2, a program to binomially combine independent tests and performance comparison with other related methods on proportional data. *BMC Bioinformatics* **10**, 443.
- Deng H-W, Lynch M (1996) Change of genetic architecture in response to sex. *Genetics*, **143**, 203-212.

- Eckert CG (2001) The loss of sex in clonal plants. *Evolutionary Ecology*, **15**, 501-520.
- Erdner DL, Richlen M, McCauley LAR, Anderson DM (2011) Diversity and dynamics of a widespread bloom of the toxic dinoflagellate *Alexandrium fundyense*. *Plos One*, **6**, e22965.
- Estrada, M, Solé, J, Anglès, S, Garcés, E (2010). The role of resting cysts in *Alexandrium minutum* population dynamics. *Deep Sea Research Part II: Topical Studies in Oceanography*, **57**, 308-321.
- Excoffier L, Lischer HEL (2010) Arlequin suite ver 3.5: a new series of programs to perform population genetics analyses under Linux and Windows. *Molecular Ecology Resources*, **10**, 564-567.
- Figueroa RI, Garcés E, Bravo I (2007) Comparative study of the life cycles of *Alexandrium tamutum* and *Alexandrium minutum* (Gonyaulacales, Dinophyceae) in culture. *Journal of Phycology*, **43**, 1039-1053.
- Figueroa RI, Garcés E, Camp J (2010) Reproductive plasticity and local adaptation in the host parasite system formed by the toxic *Alexandrium minutum* and the dinoflagellate parasite *Parvilucifera sinerae*. *Harmful Algae*, **10**, 1-8.
- Figueroa RI, Vázquez JA, Massanet A, Murado MA, Bravo I (2011) Interactive effects of salinity and temperature on planozygote and cyst formation of *Alexandrium minutum* (Dinophyceae) in culture. *Journal of Phycology*, **47**, 13-24.
- Finlay BJ, Fenchel Tom (2004) Cosmopolitan metapopulations of free-living microbial eukaryotes. *Protist*, **155**, 237-244.
- Garcés E, Bravo I, Vila M, Figueroa R. I, Maso M, Sampedro N (2004) Relationship between vegetative cells and cyst production during *Alexandrium minutum* bloom in Arenys de Mar harbour (NW Mediterranean). *Journal of Plankton Research*, **26**, 637-645.

- Gómez A, Carvalho GR (2000) Sex, parthenogenesis and genetic structure of rotifers: microsatellite analysis of contemporary and resting egg bank populations. *Molecular Ecology*, **9**, 203-214.
- Goudet J (1999) PCA-GENE, version 1.2. <http://www2.unil.ch/popgen/softwares/pcagen.htm>. (Accessed 08 April 2013).
- Goudet J (2001) Fstat, a program to estimate and test gene diversities and fixation indices (version 2.9.3.2). <http://www2.unil.ch/popgen/softwares/fstat.htm>. (Accessed 08 April 2013).
- Gsell AS, de Senerpont Domis LN, Przytulska-Bartosiewicz A, et al. (2012) Genotype-by-temperature interactions may help to maintain clonal diversity in *Asterionella formosa* (Bacillariophyceae). *Journal of Phycology*, **48**, 1197-1208.
- Hairston J, N G, Kearns CM, Ellner SP (1996) Phenotypic variation in a zooplankton egg bank. *Ecology*, **77**, 2382-2392.
- Halim, Y (1960) *Alexandrium minutum* nov. g., nov. sp., a dinoflagellate causing red water. *Vie et Milieu*, **11**, 102-105.
- Jost L (2008) G(ST) and its relatives do not measure differentiation. *Molecular Ecology*, **17**, 4015-4026.
- Lebret K, Kritzberg ES, Figueroa R, Rengefors K (2012) Genetic diversity within and genetic differentiation between blooms of a microalgal species. *Environmental Microbiology*, **14**, 2395-2404.
- Lepelletier F, Karpov SA, Le Panse S, Bigeard E, Skovgaard AA, Jeanthon C, Guillou L (2013) *Parvilucifera rostrata* sp. nov., a novel parasite in the phylum Perkinsozoa that infects the toxic dinoflagellate *Alexandrium minutum* (Dinophyceae). *Protist*, (Submitted).

- Marie D, Simon N, Guillou L, Partensky F, Vaultot D (2000). DNA, RNA analysis of phytoplankton by flow cytometry. In: Current Protocols in Cytometry. *John Wiley & Sons, Inc.***11, 12**, 1-18.
- Mauger S, Couceiro L, Valero M (2012) A simple and cost-effective method to synthesize an internal size standard amenable to use with a 5-dye system. *Prime Journals*, **2**, 40-46.
- Maynard-Smith J (1978) The evolution of sex. Cambridge University Press, London, U.K.
- Maynard-Smith J, Hoekstra R (1980). Polymorphism in a varied environment: how robust are the models? *Genetic Research*, **35**, 45-57.
- Maynard-Smith J, Smith N. H, O'Rourke M, and Spratt B. G (1993). How clonal are bacteria? *Proceedings of the National Academy of Sciences. USA*, **90**, 4384-4388.
- McCauley LAR, Erdner DL, Nagai S, Richlen ML, Anderson DM (2009) Biogeographic analysis of the globally distributed harmful algal bloom species *Alexandrium minutum* (Dinophyceae) based on rRNA gene sequences and microsatellite markers. *Journal of Phycology*, **45**, 454-463.
- McCue K, Holtsford T (1998) Seed bank influences on genetic diversity in the rare annual *Clarkia springvillensis* (Onagraceae). *American Journal of Botany*, **85**, 30-30.
- Montagnes D, Chambouvet A, Guillou L (2008) Responsibility of microzooplankton and parasite pressure for the demise of toxic dinoflagellate blooms. *Aquatic Microbial Ecology*, **53**, 211-225.
- Moon-van der Staay SY, De Wachter R, Vaultot D (2001) Oceanic 18S rDNA sequences from picoplankton reveal unsuspected eukaryotic diversity. *Nature*, **409**, 607-610.
- Nagai S, McCauley L, Yasuda N, et al. (2006) Development of microsatellite markers in the toxic dinoflagellate *Alexandrium minutum* (Dinophyceae). *Molecular Ecology Notes*, **6**, 756-758.

- Nagai S, Lian C, Yamaguchi S, et al. (2007) Microsatellite markers reveal population genetic structure of the toxic dinoflagellate *Alexandrium tamarense* (Dinophyceae) in Japanese coastal waters. *Journal of Phycology*, **43**, 43-54.
- Nei M (1987) Molecular evolutionary genetics. Columbia University Press, New York, USA.
- Norris RD (2000) Pelagic species diversity, biogeography, and evolution. *Paleobiology*, **26**, 236-258.
- Palumbi SR (1994) Reproductive isolation, genetic divergence, and speciation in the sea. *Annual Review of Ecology and Systematics*. **25**, 547-572.
- Pitcher GC, Cembella AD, Joyce LB, Larsen J, Probyn R.A, Sebastián R (2007) The dinoflagellate *Alexandrium minutum* in Cape Town harbour (South Africa): Bloom characteristics, phylogenetic analysis and toxin composition. *Harmful Algae*, **6**, 823-36.
- Probert I, Lewis J, Erard-Le Denn E (2002) Morphological details of the life history of *Alexandrium minutum* (Dinophyceae). *Cryptogamie Algologie*, **23**, 343-55.
- Richlen ML, Erdner DL, McCauley LAR, Libera K, Anderson DM (2012) Extensive genetic diversity and rapid population differentiation during blooms of *Alexandrium fundyense* (Dinophyceae) in an isolated salt pond on Cape Cod, MA, USA. *Ecology and Evolution*, **2**, 2588-2599.
- Rispe C, Pierre JS, Simon JC, Gouyon PH (1998) Models of sexual and asexual coexistence in aphids based on constraints. *Journal of Evolutionary Biology*, **11**, 685-701.
- Rynearson TA, Armbrust EV (2000) DNA fingerprinting reveals extensive genetic diversity in a field population of the centric diatom *Ditylum brightwellii*. *Limnology and Oceanography*, **45**, 1329-1340.
- Rynearson TA, Armbrust EV (2005) Maintenance of clonal diversity during a spring bloom of the centric diatom *Ditylum brightwellii*. *Molecular Ecology*, **14**:1631–1640.

- Rynearson TA, Newton JA, Armbrust EV (2006) Spring bloom development, genetic variation, and population succession in the planktonic diatom *Ditylum brightwellii*. *Limnology and Oceanography*, **51**, 1249-1261.
- Scholin CA, Anderson DM (1994) Identification of group- and strain-specific genetic markers for globally distributed *Alexandrium* (Dinophyceae). I. Rflp analysis of SSU rRNA genes. *Journal of Phycology*, **30**, 744-754.
- Silvertown J (2008) The evolutionary maintenance of sexual reproduction: evidence from the ecological distribution of asexual reproduction in clonal plants. *International journal of plant sciences*, **169**, 157-168.
- Teriokhin, A.T., De Meeûs, T., Guegan, J.F. 2007. On the power of some binomial modifications of the Bonferroni multiple test. *Zh. Obshch. Biol.* **68**, 332-340.
- Wyatt T, Jenkinson IR (1997) Notes on *Alexandrium* population dynamics. *Journal of Plankton Research*, **19**, 551-575.

Data accessibility

Data used in this study (supplementary Table S1) have been deposited at the Roscoff Culture Collection (www.sb-roscoff.fr/Phyto/RCC).

Authors' contributions

AD conceived the study, performed isolation and culture of strains, molecular data, analysis and drafted the manuscript, SM contributed to molecular analyses; EB performed isolation and culture of strains, DM performed cytometry analyses, MV participated in the design of the study, performed some statistical analysis and revised the manuscript, LG and CD coordinated the study, helped draft and revised the manuscript. All authors contributed to sample collection, read and approved the final manuscript.

Figure legends:

Figure 1: Maps of the study area showing sampling stations in the two estuaries: Penzé (PZ) and Rance (RC).

Figure 2: PCA of genetic differentiation between samples taken from the Penzé and Rance estuaries in 2010 and 2011.

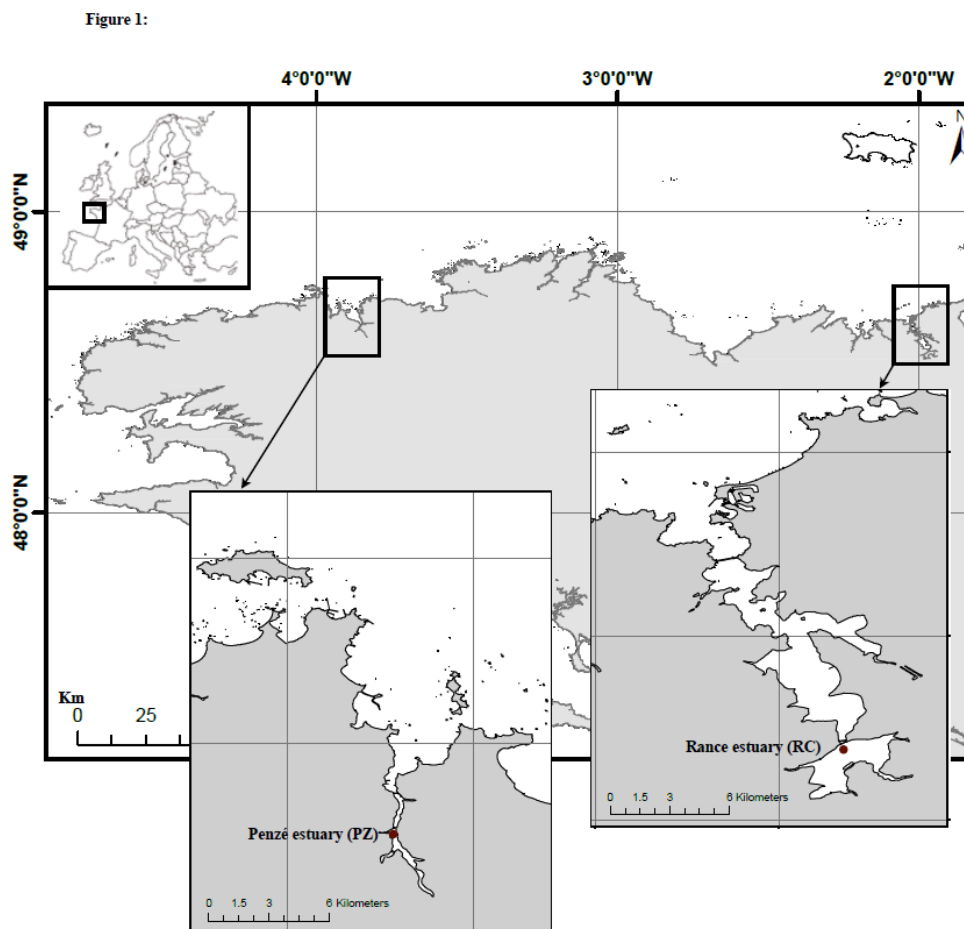


Figure 2:

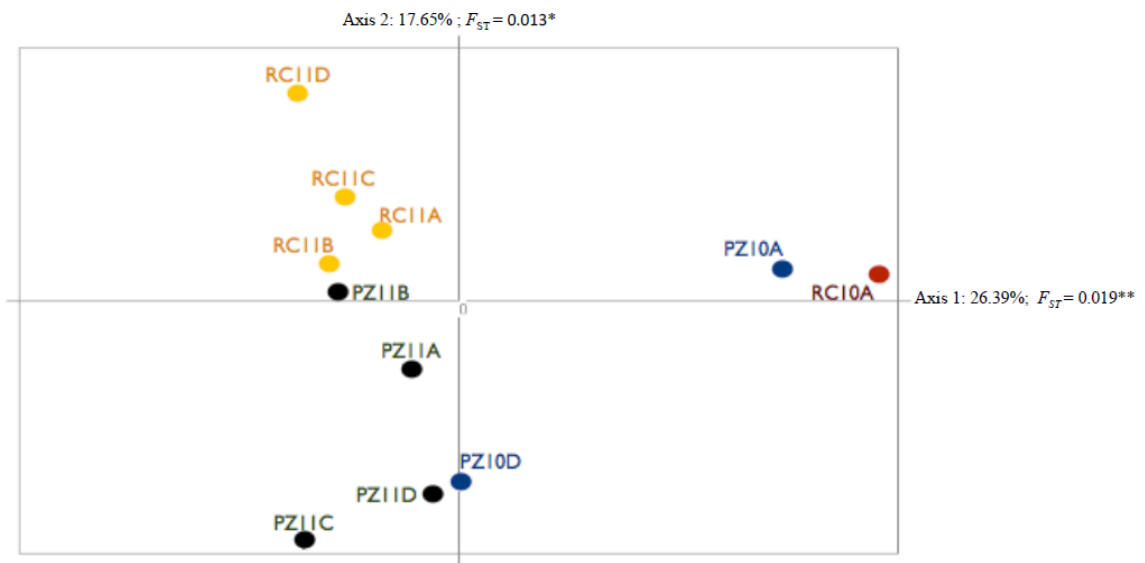


Table 1: Characteristics of the spatiotemporal sampling. Sample sizes (N) are given for strains that were isolated for culturing and for the surviving strains that were genotyped. Codes for samples: PZ for Penzé, RC for Rance; 10 for 2010 and 11 for 2011; A, B, C and D indicate respectively the different periods of the blooms: the beginning, the middle 1, the middle 2 and the end of the bloom. Cells were counted in a counting chamber using an inverted microscope (Olympus CKX41).

Site/Year	Sampling date	Sample code	Cells density x 10 ³ cells/L	Temperature of water (air temperature min./ max.) (°C)	Number of strains isolated	Number of surviving strains (%)	Number of <i>A. minutum</i> strains after screening	Number of strains genotyped
Penzé/2010	02 June	PZ10A	8	14.5 (8.6/22)	82	36 (43.9)	32	24
	30 June	PZ10D	102	19.0 (13.5/24.5)	29	16 (55.2)	09	09
	01 July	PZ10D	63	19.3 (12.2/25.9)	55	30 (54.5)	14	08
Penzé/2011	01 June	PZ11A	31	17.9 (2.7/18.6)	85	55 (64.7)	22	19
	15 June	PZ11B	88	18.0 (12.3/20.5)	93	46 (49.4)	24	14
	17 June	PZ11B	171	15.9 (8.4/16.3)	144	36 (25)	24	15
	22 June	PZ11C	402	16.0 (11.5/18)	119	49 (41.2)	32	24
	11 July	PZ11D	ND	17.5 (9/23.8)	195	30 (15.4)	26	18
Rance/2010	02 June	RC10A	36	16.3 (11.2/17.8)	65	43 (66.2)	43	40
Rance/2011	09 May	RC11A	13	15.4 (9.8/19.7)	45	26 (57.8)	19	15
	23 May	RC11B	168	16.8 (7.4/24.2)	96	55 (55.2)	40	25
	27 May	RC11C	288	17.0 (10.8/15.1)	96	57 (59.3)	38	25
	03 June	RC11D	66	18.5 (13/22.1)	83	22 (26.5)	17	10
	05 June	RC11D	106	18.8 (13.8/14.7)	53	29 (54.7)	24	19
Total					1240	530 (42.7)	364	265

Table 2: Genetic diversity estimates in *A. minutum* at each of the 11 sampling sites and dates and for each of the seven microsatellite loci. N , number of individuals genotyped in each sample; N_a , number of alleles per locus; R_a , expected allelic richness based on the smallest sample size (10); H_s , Nei's gene diversity.

Sample (N)	PZ10 A (24)	PZ10 D (17)	PZ11 A (19)	PZ11 B (29)	PZ11 C (24)	PZ11 D (18)	RC10 A (40)	RC11 A (15)	RC11 B (25)	RC11 C (25)	RC11 D (29)
Aminu22											
N	19	15	14	26	23	16	34	12	23	21	27
N_a	4	7	4	9	6	5	9	5	7	8	8
R_a	3.74	6.58	3.85	6.62	5.05	4.60	6.36	4.96	5.63	6.33	5.97
H_s	0.57	0.84	0.57	0.73	0.75	0.68	0.76	0.74	0.63	0.62	0.68
Aminu41											
N	22	16	17	27	24	17	36	12	23	19	24
N_a	10	3	4	7	3	4	10	3	6	10	5
R_a	7.93	3.00	3.68	5.29	2.67	3.82	6.63	2.98	4.74	8.26	4.00
H_s	0.84	0.69	0.64	0.71	0.56	0.68	0.77	0.59	0.63	0.85	0.62
Aminu11											
N	22	16	17	28	22	17	33	14	23	25	28
N_a	12	9	9	12	12	11	14	10	11	14	13
R_a	10.02	8.20	8.54	9.04	9.55	9.82	9.85	9.48	9.34	10.67	10.38
H_s	0.94	0.90	0.93	0.89	0.91	0.94	0.91	0.95	0.93	0.93	0.94
Aminu20											
N	19	14	10	28	19	17	24	11	21	18	23
N_a	10	9	7	17	13	10	9	5	13	13	12
R_a	8.22	8.55	7.00	12.28	11.23	8.68	6.88	4.99	10.68	11.03	9.30
H_s	0.78	0.91	0.91	0.96	0.97	0.84	0.79	0.84	0.95	0.95	0.89
Aminu43											
N	19	16	18	24	23	14	28	14	22	19	20
N_a	13	10	13	12	13	8	15	8	14	9	10
R_a	10.92	9.17	10.90	9.84	10.05	7.63	10.90	7.70	10.96	8.00	8.99
H_s	0.95	0.93	0.94	0.93	0.92	0.89	0.93	0.91	0.94	0.89	0.93
Aminu48											
N	17	15	19	25	23	18	37	15	20	25	27
N_a	11	12	11	10	8	7	14	5	8	10	9
R_a	9.82	10.96	9.18	7.71	6.69	6.36	8.74	4.78	6.73	7.74	6.54
H_s	0.94	0.96	0.87	0.83	0.83	0.78	0.85	0.64	0.80	0.85	0.68
Aminu08											
N	22	15	17	27	23	14	28	13	23	24	28
N_a	9	10	11	13	10	11	13	11	13	15	11
R_a	7.38	9.36	9.82	9.18	8.22	10.33	9.67	10.58	9.90	11.07	7.91
H_s	0.83	0.94	0.94	0.87	0.88	0.96	0.91	0.97	0.88	0.93	0.83
Mean over loci											
N_a	9.86	8.57	8.43	11.43	9.29	8.00	12.00	6.71	10.29	11.29	9.71
(SE)	0.30	0.34	0.42	0.28	0.41	0.35	0.22	0.44	0.32	0.24	0.28
R_a	8.29	7.97	7.57	8.56	7.64	7.32	8.43	6.49	8.28	9.01	7.58
(SE)	0.29	0.32	0.38	0.27	0.40	0.34	0.21	0.43	0.31	0.21	0.29
H_s	0.84	0.88	0.83	0.85	0.83	0.82	0.85	0.81	0.82	0.86	0.79
(SE)	0.16	0.11	0.19	0.11	0.17	0.14	0.09	0.19	0.17	0.13	0.17

Table 3: Multilocus measurements of linkage disequilibrium using \bar{r}_d (Agapow and Burt 2001).

Sample (N)	PZ10A (24)	PZ10D (17)	PZ11A (19)	PZ11B (29)	PZ11C (24)	PZ11D (18)	RC10A (40)	RC11A (15)	RC11B (25)	RC11C (25)	RC11D (29)
\bar{r}_d	-0.008	0.068	-0.034	-0.017	0.037	0.005	0.003	0.027	-0.037	-0.049	0.009
P-value	0.566	0.047	0.870	0.730	0.063	0.416	0.423	0.240	0.902	0.971	0.348

Table 4: Spatial (A) and temporal (B) analyses of bloom events

A: Spatial AMOVA: Variation among bloom phases between the Penzé and Rance sites sampled in 2011 ($F_{st} = 0.05$. $P < 10^{-5}$)

Source of variation	df	Sum of squares	Variance component	Percentage variation (%)	P-value
Between the Penzé and Rance sites sampled in 2011	1	13.91	0.04	1.23	0.008
Among bloom phases within site	6	44.51	0.12	3.87	0.002
Within bloom phase	318	896.08	2.82	94.88	
Total		954.49	2.97		

B: Temporal AMOVA: Variation among bloom phases between years 2010 and 2011 at Penzé site ($F_{st} = 0.14$. $p < 10^{-5}$)

Source of variation	df	Sum of squares	Variance component	Percentage variation (%)	P-value
Between years 2010 and 2011 in Penzé	1	41.24	0.33	10.01	$p < 10^{-5}$
Among bloom phases within year	4	33.04	0.14	4.27	$p < 10^{-5}$
Within bloom phase	226	648.12	2.86	85.72	
Total		722.41	3.34		

SUPPORTING INFORMATION FOR:

SPATIOTEMPORAL CHANGES IN THE GENETIC DIVERSITY OF HARMFUL ALGAL BLOOMS CAUSED BY THE TOXIC DINOFLAGELLATE *ALEXANDRIUM MINUTUM*

Aliou Dia, Laure Guillou, Stéphane Mauger, Estelle Bigeard, Dominique Marie, Myriam Valero, Christophe Destombe

UPMC Paris VI, UMR 7144, Adaptation et diversité en milieu marin, Station Biologique de Roscoff, Place Georges Teissier, CS 90074, 29688 Roscoff, France.

CNRS, UMR 7144, Adaptation et diversité en milieu marin, Station Biologique de Roscoff, Place Georges Teissier, CS 90074, 29688 Roscoff, France

Figure S1. Quantification of DNA in *Alexandrium minutum* cultures in comparison with nuclei isolated from human blood cells (HBC, 6.4 Mbp), after staining with propidium iodide in PBS buffer. HBC and *A. minutum* are discriminated on the forward scatter (X-axis, logarithmic scale), a proxy of size, versus red fluorescence (Y-axis, linear scale) dot plot (A). Quantification of DNA (X-axis, linear scale) by fluorescence in two monoclonal strains (B) and (C).

Figure S2. Resolving power of the microsatellite marker set to discriminate the maximum clonal diversity available in the data set.

Supplementary Tables (3)

Table S1. Roscoff Culture Collection (RCC) number, origin, population code and date of isolation of strains used in this study. RCC web site: www.sb-roscoff.fr/Phyto/RCC.

Strain number	Site	Population code	Date
RCC 3144	Penzé	PZ10A	02-June-10
RCC 3145	Penzé	PZ10A	02-June-10
RCC 3146	Penzé	PZ10A	02-June-10
RCC 3147	Penzé	PZ10A	02-June-10
RCC 3148	Penzé	PZ10A	02-June-10

RCC 3149	Penzé	PZ10A	02-June-10
RCC 3150	Penzé	PZ10A	02-June-10
RCC 3151	Penzé	PZ10A	02-June-10
RCC 3152	Penzé	PZ10A	02-June-10
RCC 3153	Penzé	PZ10A	02-June-10
RCC 3154	Penzé	PZ10A	02-June-10
RCC 3155	Penzé	PZ10A	02-June-10
RCC 3156	Penzé	PZ10A	02-June-10
RCC 3157	Penzé	PZ10A	02-June-10
RCC 3158	Penzé	PZ10A	02-June-10
RCC 3159	Penzé	PZ10A	02-June-10
RCC 3160	Penzé	PZ10A	02-June-10
RCC 3161	Penzé	PZ10A	02-June-10
RCC 3162	Penzé	PZ10A	02-June-10
RCC 3163	Penzé	PZ10A	02-June-10
RCC 3164	Penzé	PZ10A	02-June-10
RCC 3165	Penzé	PZ10A	02-June-10
RCC 3166	Penzé	PZ10A	02-June-10
RCC 3167	Penzé	PZ10A	02-June-10
RCC 3168	Penzé	PZ10D	30-June-10
RCC 3169	Penzé	PZ10D	30-June-10
RCC 3170	Penzé	PZ10D	30-June-10
RCC 3171	Penzé	PZ10D	30-June-10
RCC 3172	Penzé	PZ10D	30-June-10
RCC 3173	Penzé	PZ10D	30-June-10
RCC 3174	Penzé	PZ10D	30-June-10
RCC 3175	Penzé	PZ10D	30-June-10
RCC 3176	Penzé	PZ10D	30-June-10
RCC 3177	Penzé	PZ10D	01-July-10
RCC 3178	Penzé	PZ10D	01-July-10
RCC 3179	Penzé	PZ10D	01-July-10
RCC 3180	Penzé	PZ10D	01-July-10
RCC 3181	Penzé	PZ10D	01-July-10
RCC 3182	Penzé	PZ10D	01-July-10
RCC 3183	Penzé	PZ10D	01-July-10
RCC 3023	Penzé	PZ10D	01-July-10
RCC 3249	Penzé	PZ11A	01-June-11
RCC 3250	Penzé	PZ11A	01-June-11
RCC 3251	Penzé	PZ11A	01-June-11
RCC 3252	Penzé	PZ11A	01-June-11
RCC 3253	Penzé	PZ11A	01-June-11
RCC 3254	Penzé	PZ11A	01-June-11
RCC 3255	Penzé	PZ11A	01-June-11
RCC 3256	Penzé	PZ11A	01-June-11
RCC 3257	Penzé	PZ11A	01-June-11
RCC 3258	Penzé	PZ11A	01-June-11
RCC 3259	Penzé	PZ11A	01-June-11
RCC 3260	Penzé	PZ11A	01-June-11

RCC 3261	Penzé	PZ11A	01-June-11
RCC 3262	Penzé	PZ11A	01-June-11
RCC 3263	Penzé	PZ11A	01-June-11
RCC 3264	Penzé	PZ11A	01-June-11
RCC 3265	Penzé	PZ11A	01-June-11
RCC 3266	Penzé	PZ11A	01-June-11
RCC 3267	Penzé	PZ11A	01-June-11
RCC 3297	Penzé	PZ11B	15-June-11
RCC 3298	Penzé	PZ11B	15-June-11
RCC 3299	Penzé	PZ11B	15-June-11
RCC 3300	Penzé	PZ11B	15-June-11
RCC 3301	Penzé	PZ11B	15-June-11
RCC 3302	Penzé	PZ11B	15-June-11
RCC 3303	Penzé	PZ11B	15-June-11
RCC 3304	Penzé	PZ11B	15-June-11
RCC 3305	Penzé	PZ11B	15-June-11
RCC 3306	Penzé	PZ11B	15-June-11
RCC 3307	Penzé	PZ11B	15-June-11
RCC 3308	Penzé	PZ11B	15-June-11
RCC 3309	Penzé	PZ11B	15-June-11
RCC 3310	Penzé	PZ11B	15-June-11
RCC 3311	Penzé	PZ11B	17-June-11
RCC 3312	Penzé	PZ11B	17-June-11
RCC 3313	Penzé	PZ11B	17-June-11
RCC 3314	Penzé	PZ11B	17-June-11
RCC 3315	Penzé	PZ11B	17-June-11
RCC 3316	Penzé	PZ11B	17-June-11
RCC 3317	Penzé	PZ11B	17-June-11
RCC 3318	Penzé	PZ11B	17-June-11
RCC 3319	Penzé	PZ11B	17-June-11
RCC 3320	Penzé	PZ11B	17-June-11
RCC 3321	Penzé	PZ11B	17-June-11
RCC 3322	Penzé	PZ11B	17-June-11
RCC 3323	Penzé	PZ11B	17-June-11
RCC 3324	Penzé	PZ11B	17-June-11
RCC 3325	Penzé	PZ11B	17-June-11
RCC 3326	Penzé	PZ11C	22-June-11
RCC 3327	Penzé	PZ11C	22-June-11
RCC 3328	Penzé	PZ11C	22-June-11
RCC 3329	Penzé	PZ11C	22-June-11
RCC 3330	Penzé	PZ11C	22-June-11
RCC 3331	Penzé	PZ11C	22-June-11
RCC 3332	Penzé	PZ11C	22-June-11
RCC 3333	Penzé	PZ11C	22-June-11
RCC 3334	Penzé	PZ11C	22-June-11
RCC 3335	Penzé	PZ11C	22-June-11
RCC 3336	Penzé	PZ11C	22-June-11
RCC 3337	Penzé	PZ11C	22-June-11

RCC 3338	Penzé	PZ11C	22-June-11
RCC 3339	Penzé	PZ11C	22-June-11
RCC 3340	Penzé	PZ11C	22-June-11
RCC 3341	Penzé	PZ11C	22-June-11
RCC 3342	Penzé	PZ11C	22-June-11
RCC 3343	Penzé	PZ11C	22-June-11
RCC 3344	Penzé	PZ11C	22-June-11
RCC 3345	Penzé	PZ11C	22-June-11
RCC 3346	Penzé	PZ11C	22-June-11
RCC 3347	Penzé	PZ11C	22-June-11
RCC 3348	Penzé	PZ11C	22-June-11
RCC 3349	Penzé	PZ11C	22-June-11
RCC 3350	Penzé	PZ11D	11-July-11
RCC 3351	Penzé	PZ11D	11-July-11
RCC 3352	Penzé	PZ11D	11-July-11
RCC 3353	Penzé	PZ11D	11-July-11
RCC 3354	Penzé	PZ11D	11-July-11
RCC 3355	Penzé	PZ11D	11-July-11
RCC 3356	Penzé	PZ11D	11-July-11
RCC 3357	Penzé	PZ11D	11-July-11
RCC 3358	Penzé	PZ11D	11-July-11
RCC 3359	Penzé	PZ11D	11-July-11
RCC 3360	Penzé	PZ11D	11-July-11
RCC 3361	Penzé	PZ11D	11-July-11
RCC 3362	Penzé	PZ11D	11-July-11
RCC 3363	Penzé	PZ11D	11-July-11
RCC 3364	Penzé	PZ11D	11-July-11
RCC 3365	Penzé	PZ11D	11-July-11
RCC 3366	Penzé	PZ11D	11-July-11
RCC 3367	Penzé	PZ11D	11-July-11
RCC 3105	Rance	RC10A	02-June-10
RCC 3106	Rance	RC10A	02-June-10
RCC 3107	Rance	RC10A	02-June-10
RCC 3108	Rance	RC10A	02-June-10
RCC 3109	Rance	RC10A	02-June-10
RCC 3110	Rance	RC10A	02-June-10
RCC 3111	Rance	RC10A	02-June-10
RCC 3112	Rance	RC10A	02-June-10
RCC 3113	Rance	RC10A	02-June-10
RCC 3022	Rance	RC10A	02-June-10
RCC 3114	Rance	RC10A	02-June-10
RCC 3115	Rance	RC10A	02-June-10
RCC 3116	Rance	RC10A	02-June-10
RCC 3117	Rance	RC10A	02-June-10
RCC 3118	Rance	RC10A	02-June-10
RCC 3119	Rance	RC10A	02-June-10
RCC 3120	Rance	RC10A	02-June-10
RCC 3121	Rance	RC10A	02-June-10

RCC 3122	Rance	RC10A	02-June-10
RCC 3123	Rance	RC10A	02-June-10
RCC 3124	Rance	RC10A	02-June-10
RCC 3125	Rance	RC10A	02-June-10
RCC 3126	Rance	RC10A	02-June-10
RCC 3127	Rance	RC10A	02-June-10
RCC 3128	Rance	RC10A	02-June-10
RCC 3129	Rance	RC10A	02-June-10
RCC 3130	Rance	RC10A	02-June-10
RCC 3131	Rance	RC10A	02-June-10
RCC 3132	Rance	RC10A	02-June-10
RCC 3133	Rance	RC10A	02-June-10
RCC 3134	Rance	RC10A	02-June-10
RCC 3135	Rance	RC10A	02-June-10
RCC 3136	Rance	RC10A	02-June-10
RCC 3137	Rance	RC10A	02-June-10
RCC 3138	Rance	RC10A	02-June-10
RCC 3139	Rance	RC10A	02-June-10
RCC 3140	Rance	RC10A	02-June-10
RCC 3141	Rance	RC10A	02-June-10
RCC 3142	Rance	RC10A	02-June-10
RCC 3143	Rance	RC10A	02-June-10
RCC 3184	Rance	RC11A	09-May-11
RCC 3185	Rance	RC11A	09-May-11
RCC 3186	Rance	RC11A	09-May-11
RCC 3187	Rance	RC11A	09-May-11
RCC 3188	Rance	RC11A	09-May-11
RCC 3189	Rance	RC11A	09-May-11
RCC 3190	Rance	RC11A	09-May-11
RCC 3191	Rance	RC11A	09-May-11
RCC 3192	Rance	RC11A	09-May-11
RCC 3193	Rance	RC11A	09-May-11
RCC 3194	Rance	RC11A	09-May-11
RCC 3195	Rance	RC11A	09-May-11
RCC 3196	Rance	RC11A	09-May-11
RCC 3197	Rance	RC11A	09-May-11
RCC 3198	Rance	RC11A	09-May-11
RCC 3199	Rance	RC11B	23-May-11
RCC 3200	Rance	RC11B	23-May-11
RCC 3201	Rance	RC11B	23-May-11
RCC 3202	Rance	RC11B	23-May-11
RCC 3203	Rance	RC11B	23-May-11
RCC 3204	Rance	RC11B	23-May-11
RCC 3205	Rance	RC11B	23-May-11
RCC 3206	Rance	RC11B	23-May-11
RCC 3207	Rance	RC11B	23-May-11
RCC 3208	Rance	RC11B	23-May-11
RCC 3209	Rance	RC11B	23-May-11

RCC 3210	Rance	RC11B	23-May-11
RCC 3211	Rance	RC11B	23-May-11
RCC 3212	Rance	RC11B	23-May-11
RCC 3213	Rance	RC11B	23-May-11
RCC 3214	Rance	RC11B	23-May-11
RCC 3215	Rance	RC11B	23-May-11
RCC 3216	Rance	RC11B	23-May-11
RCC 3217	Rance	RC11B	23-May-11
RCC 3218	Rance	RC11B	23-May-11
RCC 3219	Rance	RC11B	23-May-11
RCC 3220	Rance	RC11B	23-May-11
RCC 3221	Rance	RC11B	23-May-11
RCC 3222	Rance	RC11B	23-May-11
RCC 3223	Rance	RC11B	23-May-11
RCC 3224	Rance	RC11C	27-May-11
RCC 3225	Rance	RC11C	27-May-11
RCC 3226	Rance	RC11C	27-May-11
RCC 3227	Rance	RC11C	27-May-11
RCC 3228	Rance	RC11C	27-May-11
RCC 3229	Rance	RC11C	27-May-11
RCC 3230	Rance	RC11C	27-May-11
RCC 3231	Rance	RC11C	27-May-11
RCC 3232	Rance	RC11C	27-May-11
RCC 3233	Rance	RC11C	27-May-11
RCC 3234	Rance	RC11C	27-May-11
RCC 3235	Rance	RC11C	27-May-11
RCC 3236	Rance	RC11C	27-May-11
RCC 3237	Rance	RC11C	27-May-11
RCC 3238	Rance	RC11C	27-May-11
RCC 3239	Rance	RC11C	27-May-11
RCC 3240	Rance	RC11C	27-May-11
RCC 3241	Rance	RC11C	27-May-11
RCC 3242	Rance	RC11C	27-May-11
RCC 3243	Rance	RC11C	27-May-11
RCC 3244	Rance	RC11C	27-May-11
RCC 3245	Rance	RC11C	27-May-11
RCC 3246	Rance	RC11C	27-May-11
RCC 3247	Rance	RC11C	27-May-11
RCC 3248	Rance	RC11C	27-May-11
RCC 3268	Rance	RC11D	03-June-11
RCC 3269	Rance	RC11D	03-June-11
RCC 3270	Rance	RC11D	03-June-11
RCC 3271	Rance	RC11D	03-June-11
RCC 3272	Rance	RC11D	03-June-11
RCC 3273	Rance	RC11D	03-June-11
RCC 3274	Rance	RC11D	03-June-11
RCC 3275	Rance	RC11D	03-June-11
RCC 3276	Rance	RC11D	03-June-11

RCC 3277	Rance	RC11D	03-June-11
RCC 3278	Rance	RC11D	05-June-11
RCC 3279	Rance	RC11D	05-June-11
RCC 3280	Rance	RC11D	05-June-11
RCC 3281	Rance	RC11D	05-June-11
RCC 3282	Rance	RC11D	05-June-11
RCC 3283	Rance	RC11D	05-June-11
RCC 3284	Rance	RC11D	05-June-11
RCC 3285	Rance	RC11D	05-June-11
RCC 3286	Rance	RC11D	05-June-11
RCC 3287	Rance	RC11D	05-June-11
RCC 3288	Rance	RC11D	05-June-11
RCC 3289	Rance	RC11D	05-June-11
RCC 3290	Rance	RC11D	05-June-11
RCC 3291	Rance	RC11D	05-June-11
RCC 3292	Rance	RC11D	05-June-11
RCC 3293	Rance	RC11D	05-June-11
RCC 3294	Rance	RC11D	05-June-11
RCC 3295	Rance	RC11D	05-June-11
RCC 3296	Rance	RC11D	05-June-11

Table S2. Microsatellite data amplified on 265 individual strains at seven loci. Population codes are given in Table 1.

Individuals	Sample codes	Aminu22	Aminu41	Aminu11	Aminu20	Aminu43	Aminu48	Aminu08
PZ374	PZ10A	199	202	255	0	201	215	185
PZ352	PZ10A	199	200	228	279	201	0	190
PZ330	PZ10A	197	164	240	248	0	0	180
PZ350	PZ10A	197	202	228	279	0	176	185
PZ344	PZ10A	197	200	228	0	215	217	185
PZ341	PZ10A	197	232	248	248	230	234	185
PZ362	PZ10A	197	200	238	279	188	0	190
PZ339	PZ10A	197	232	0	0	202	0	190
PZ351	PZ10A	197	202	236	250	197	214	190
PZ359	PZ10A	197	162	240	279	188	0	199
PZ331	PZ10A	195	202	236	0	205	240	187
PZ360	PZ10A	179	0	236	279	221	0	190
PZ353	PZ10A	0	218	0	279	220	0	185
PZ345	PZ10A	0	0	287	0	188	252	185
PZ355	PZ10A	0	232	248	279	221	176	190
PZ356	PZ10A	0	207	238	279	197	214	190
PZ340	PZ10A	0	163	248	279	188	176	197
PZ333	PZ10A	195	202	237	236	200	239	187
PZ334	PZ10A	197	200	238	253	204	239	189
PZ337	PZ10A	197	202	255	273	189	240	191
PZ338	PZ10A	199	202	239	269	0	242	0
PZ348	PZ10A	199	204	242	265	0	240	189
PZ354	PZ10A	197	206	229	267	187	238	0
PZ369	PZ10A	197	202	267	247	0	206	174
PZ482	PZ10D	201	200	244	271	197	239	179
PZ484	PZ10D	197	204	229	261	204	0	184
PZ485	PZ10D	199	204	225	263	200	231	216
PZ487	PZ10D	199	200	225	0	211	232	226
PZ488	PZ10D	199	204	225	248	200	234	216
PZ489	PZ10D	0	0	225	231	0	210	0
PZ491	PZ10D	197	204	239	261	197	248	0
PZ492	PZ10D	197	200	249	251	200	0	187
PZ493	PZ10D	168	202	240	0	187	228	220
PZ520	PZ10D	199	200	242	260	190	240	185
PZ521	PZ10D	197	200	252	262	202	242	194
PZ524	PZ10D	195	202	242	248	205	239	185
PZ514	PZ10D	195	202	258	0	197	239	190
PZ509	PZ10D	182	202	242	261	198	225	190
PZ500	PZ10D	179	202	240	261	206	218	187
PZ516	PZ10D	0	200	0	279	206	229	199

PZ522	PZ10D	199	200	240	263	187	240	216
PZ579	PZ11A	182	200	228	0	204	239	0
PZ594	PZ11A	197	202	228	248	199	234	194
PZ582	PZ11A	197	200	228	273	202	239	190
PZ591	PZ11A	197	202	237	0	194	239	187
PZ584	PZ11A	197	202	257	259	196	239	185
PZ593	PZ11A	197	200	248	0	202	237	179
PZ587	PZ11A	199	202	236	0	201	239	190
PZ589	PZ11A	199	202	259	261	209	244	185
PZ583	PZ11A	199	200	242	0	207	239	185
PZ572	PZ11A	197	200	257	261	204	256	234
PZ575	PZ11A	0	0	240	0	202	235	187
PZ577	PZ11A	0	206	0	265	171	242	186
PZ578	PZ11A	0	0	239	0	206	239	217
PZ580	PZ11A	197	202	242	253	197	236	225
PZ581	PZ11A	197	202	237	237	202	240	189
PZ586	PZ11A	0	202	259	261	208	244	189
PZ590	PZ11A	0	155	240	0	0	229	187
PZ595	PZ11A	210	200	236	265	204	234	0
PZ597	PZ11A	197	200	0	0	198	241	191
PZ689	PZ11B	197	202	239	269	0	251	179
PZ691	PZ11B	197	200	229	267	196	239	210
PZ696	PZ11B	194	202	259	259	198	239	0
PZ697	PZ11B	197	200	237	270	200	242	187
PZ701	PZ11B	195	202	239	274	196	238	189
PZ704	PZ11B	195	200	257	261	197	239	187
PZ708	PZ11B	199	200	229	261	197	239	226
PZ711	PZ11B	197	0	242	263	198	241	184
PZ712	PZ11B	0	176	242	259	204	241	197
PZ714	PZ11B	195	196	229	265	212	210	179
PZ715	PZ11B	195	202	248	253	206	218	0
PZ716	PZ11B	197	202	248	283	204	240	200
PZ719	PZ11B	197	202	239	253	204	0	187
PZ721	PZ11B	197	200	239	264	201	240	201
PZ742	PZ11B	197	200	239	262	202	240	190
PZ743	PZ11B	199	202	229	0	200	240	189
PZ749	PZ11B	212	202	237	261	204	239	187
PZ959	PZ11B	197	196	248	261	206	0	189
PZ960	PZ11B	197	200	229	265	202	246	189
PZ961	PZ11B	193	202	257	257	210	240	189
PZ962	PZ11B	195	200	223	248	0	246	187
PZ963	PZ11B	197	202	238	248	204	240	211
PZ964	PZ11B	197	232	227	271	0	240	187
PZ965	PZ11B	0	223	244	265	202	240	184

PZ966	PZ11B	197	202	248	273	0	0	198
PZ967	PZ11B	0	0	0	274	208	240	208
PZ968	PZ11B	192	202	252	269	194	248	189
PZ969	PZ11B	196	210	229	279	200	0	189
PZ970	PZ11B	200	200	229	279	0	246	189
PZ788	PZ11C	200	200	236	0	198	239	190
PZ770	PZ11C	199	200	248	258	188	240	187
PZ753	PZ11C	199	202	228	253	205	242	190
PZ761	PZ11C	197	202	257	263	201	237	201
PZ764	PZ11C	195	202	0	264	203	240	185
PZ789	PZ11C	195	200	259	0	198	242	187
PZ754	PZ11C	190	200	236	267	204	239	174
PZ757	PZ11C	195	200	237	259	191	239	189
PZ758	PZ11C	195	200	226	269	204	242	184
PZ759	PZ11C	199	202	242	263	0	0	0
PZ762	PZ11C	195	202	229	267	208	239	187
PZ766	PZ11C	199	200	242	269	202	239	187
PZ767	PZ11C	0	202	0	265	212	239	184
PZ771	PZ11C	199	202	229	0	200	239	189
PZ773	PZ11C	197	200	229	273	198	233	189
PZ775	PZ11C	195	204	229	259	197	231	192
PZ777	PZ11C	199	200	242	257	208	241	225
PZ778	PZ11C	197	202	229	261	206	241	198
PZ780	PZ11C	204	200	236	0	200	241	225
PZ781	PZ11C	195	200	228	261	208	239	189
PZ782	PZ11C	199	202	238	270	204	242	189
PZ784	PZ11C	197	200	229	0	198	256	189
PZ785	PZ11C	199	202	244	270	198	240	187
PZ787	PZ11C	199	202	239	271	204	242	184
PZ665	PZ11D	199	210	242	248	209	242	0
PZ661	PZ11D	199	202	253	248	192	239	187
PZ645	PZ11D	199	202	228	248	207	237	190
PZ648	PZ11D	197	200	228	248	197	239	0
PZ682	PZ11D	197	202	252	0	203	239	0
PZ643	PZ11D	197	202	244	270	200	239	190
PZ679	PZ11D	197	200	228	254	207	240	207
PZ660	PZ11D	183	200	248	248	0	239	227
PZ655	PZ11D	0	202	0	248	0	236	190
PZ637	PZ11D	197	200	239	248	200	229	233
PZ639	PZ11D	198	0	237	269	199	239	229
PZ640	PZ11D	199	200	255	253	200	229	211
PZ641	PZ11D	197	202	242	257	204	242	221
PZ644	PZ11D	199	200	239	269	200	239	189
PZ646	PZ11D	197	200	248	261	204	229	0
PZ647	PZ11D	207	200	242	271	0	239	187

PZ658	PZ11D	0	162	238	263	0	260	237
PZ683	PZ11D	197	210	229	274	204	240	185
RC275	RC10A	0	0	208	279	214	214	0
RC277	RC10A	195	200	229	261	202	239	192
RC280	RC10A	207	202	238	237	175	235	184
RC281	RC10A	197	200	223	0	202	241	175
RC283	RC10A	197	204	229	255	202	250	189
RC297	RC10A	197	215	249	271	202	211	213
RC304	RC10A	182	226	251	0	0	231	213
RC322	RC10A	183	199	224	259	175	0	187
RC317	RC10A	202	202	238	0	0	176	205
RC307	RC10A	197	200	238	248	0	0	0
RC321	RC10A	197	204	236	0	194	0	0
RC271	RC10A	197	200	248	279	188	176	0
RC293	RC10A	197	210	242	261	198	240	0
RC323	RC10A	197	200	0	279	180	217	180
RC301	RC10A	197	200	278	0	0	226	185
RC316	RC10A	197	202	244	0	0	214	187
RC311	RC10A	197	202	248	248	188	176	199
RC310	RC10A	197	200	0	246	188	180	205
RC315	RC10A	197	202	0	0	0	240	205
RC296	RC10A	197	200	240	248	0	214	213
RC325	RC10A	197	200	278	279	184	176	230
RC327	RC10A	195	202	240	279	221	176	0
RC295	RC10A	195	202	228	248	0	226	0
RC298	RC10A	195	200	248	0	0	240	0
RC305	RC10A	195	202	238	0	198	181	185
RC313	RC10A	195	200	248	248	0	214	205
RC308	RC10A	195	0	0	0	0	240	205
RC303	RC10A	193	200	0	0	201	181	185
RC314	RC10A	193	0	0	0	217	214	190
RC324	RC10A	193	204	238	279	188	176	205
RC328	RC10A	190	200	238	279	180	176	185
RC287	RC10A	182	200	0	265	213	176	0
RC300	RC10A	182	0	238	248	221	236	0
RC282	RC10A	182	181	248	279	0	176	199
RC302	RC10A	156	218	240	0	203	226	0
RC294	RC10A	0	202	236	248	196	214	0
RC273	RC10A	0	210	278	279	188	176	190
RC292	RC10A	0	200	223	0	201	214	197
RC320	RC10A	0	223	248	0	188	176	199
RC326	RC10A	0	210	223	0	220	176	205
RC913	RC11A	195	200	244	261	0	237	189
RC915	RC11A	193	0	229	0	200	240	221
RC922	RC11A	193	202	229	259	196	240	185

RC925	RC11A	200	200	239	259	196	231	208
RC931	RC11A	197	202	239	255	206	240	191
RC937	RC11A	197	204	248	261	201	240	189
RC938	RC11A	197	202	242	269	200	243	184
RC939	RC11A	195	200	238	261	193	240	206
RC919	RC11A	197	202	236	259	198	240	185
RC921	RC11A	0	200	253	248	203	237	187
RC926	RC11A	0	200	250	248	205	239	0
RC927	RC11A	197	200	237	0	205	239	0
RC930	RC11A	197	200	238	0	205	240	172
RC932	RC11A	199	0	0	0	203	240	213
RC934	RC11A	0	0	238	248	203	240	210
RC1003	RC11B	197	200	248	253	202	0	188
RC1013	RC11B	197	200	239	268	204	238	187
RC1014	RC11B	0	202	239	271	200	240	225
RC1016	RC11B	199	200	0	258	200	239	187
RC974	RC11B	197	202	236	0	200	240	224
RC975	RC11B	197	200	238	265	198	328	187
RC978	RC11B	199	202	229	263	201	0	0
RC979	RC11B	200	200	229	255	0	0	216
RC980	RC11B	197	200	238	253	0	240	189
RC981	RC11B	197	200	263	278	195	240	187
RC982	RC11B	195	200	245	269	200	242	187
RC983	RC11B	197	202	239	261	202	242	187
RC984	RC11B	197	200	239	261	207	0	0
RC986	RC11B	197	210	244	269	202	240	197
RC987	RC11B	199	202	240	252	198	240	184
RC988	RC11B	195	196	229	0	191	236	216
RC992	RC11B	197	200	237	259	0	240	187
RC999	RC11B	197	202	237	261	209	240	205
RC1008	RC11B	197	200	238	258	203	239	172
RC1001	RC11B	197	162	244	0	205	239	185
RC1005	RC11B	197	200	240	258	198	244	190
RC1015	RC11B	191	200	0	0	218	230	230
RC994	RC11B	188	0	248	259	194	239	230
RC991	RC11B	180	0	229	269	197	0	187
RC1011	RC11B	0	208	255	273	203	239	185
RC1019	RC11C	194	223	239	0	0	242	199
RC1020	RC11C	0	200	242	0	0	258	187
RC1021	RC11C	197	202	236	259	198	242	184
RC1022	RC11C	197	202	257	267	202	240	216
RC1024	RC11C	197	202	237	261	200	242	201
RC1026	RC11C	197	196	237	273	0	240	206
RC1028	RC11C	0	200	198	261	204	240	195
RC1032	RC11C	0	212	224	0	196	238	184

RC1034	RC11C	197	218	228	275	202	226	202
RC1040	RC11C	229	0	230	0	202	233	189
RC1042	RC11C	197	200	237	255	197	233	189
RC1043	RC11C	197	200	239	261	0	242	187
RC1044	RC11C	200	200	237	255	200	247	191
RC1047	RC11C	197	0	248	251	202	238	176
RC1049	RC11C	0	180	237	263	196	238	187
RC1050	RC11C	197	0	229	269	200	242	164
RC1055	RC11C	197	0	229	276	200	238	216
RC1059	RC11C	197	197	255	0	204	240	216
RC1061	RC11C	215	0	239	0	0	244	175
RC1062	RC11C	197	0	239	265	193	218	187
RC1035	RC11C	195	204	252	0	197	242	185
RC1036	RC11C	183	210	236	261	0	242	172
RC1056	RC11C	206	200	253	253	205	242	0
RC1039	RC11C	197	202	242	253	207	239	187
RC1060	RC11C	195	202	252	258	202	240	187
RC854	RC11D	197	202	248	0	0	242	187
RC855	RC11D	197	224	241	260	204	240	189
RC857	RC11D	197	200	237	265	0	238	194
RC858	RC11D	0	0	243	0	202	235	195
RC859	RC11D	196	0	229	267	202	0	180
RC860	RC11D	198	202	255	261	196	240	0
RC861	RC11D	197	0	255	261	196	240	190
RC863	RC11D	195	202	239	267	201	240	190
RC864	RC11D	197	202	237	285	0	240	185
RC867	RC11D	197	0	239	267	0	257	187
RC873	RC11D	197	200	257	0	0	240	187
RC874	RC11D	195	200	248	267	199	240	187
RC875	RC11D	207	202	259	261	204	240	180
RC876	RC11D	202	202	0	0	204	0	190
RC877	RC11D	197	202	251	259	191	240	187
RC878	RC11D	200	201	237	253	0	264	190
RC880	RC11D	197	202	238	238	0	242	227
RC881	RC11D	197	202	238	271	208	237	187
RC884	RC11D	195	202	257	267	204	240	187
RC885	RC11D	197	202	237	261	0	240	222
RC889	RC11D	0	204	243	261	201	228	179
RC894	RC11D	197	200	229	251	193	240	187
RC895	RC11D	196	200	239	262	193	240	187
RC897	RC11D	196	200	243	262	201	242	185
RC898	RC11D	195	200	237	261	0	240	185
RC883	RC11D	197	202	236	0	205	239	190
RC886	RC11D	197	202	236	0	199	240	190

RC887	RC11D	191	200	242	255	205	239	174
RC882	RC11D	197	0	236	255	197	239	187

Table S3: Pairwise differentiation between the 11 populations of *Alexandrium minutum*. $F_{st}(\theta)$ values are given above diagonal and Jost's D_{est} below diagonal. Significant F_{st} values (1000 permutations) are depicted in bold. *: F_{st} values that remain significant after a Bonferroni correction. Population codes are given in Table 1.

	PZ10A	PZ10D	PZ11A	PZ11B	PZ11C	PZ11D	RC10A	RC11A	RC11B	RC11C	RC11D
PZ10A		0.0396	0.0265	0.0378*	0.0639*	0.0403	0.0161	0.0577	0.0456*	0.0443*	0.0486*
PZ10D	<i>0.3228</i>		0.0124	0.0247	0.0170	0.0122	0.0495*	0.0281	0.0234	0.0254	0.0495*
PZ11A	<i>0.1847</i>	<i>0.2007</i>		0.0073	0.0211	0.0019	0.0536*	0.0331	0.0100	0.0104	0.0236
PZ11B	<i>0.2748</i>	<i>0.2279</i>	<i>0.0929</i>		0.0102	0.0234	0.0522*	0.0062	0.0008	0.0059	0.0103
PZ11C	<i>0.3810</i>	<i>0.2206</i>	<i>0.1694</i>	<i>0.0576</i>		0.0259	0.0770*	0.0401	0.0260	0.0429*	0.0534*
PZ11D	<i>0.2135</i>	<i>0.2096</i>	<i>0.0956</i>	<i>0.2102</i>	<i>0.1968</i>		0.0623*	0.0318	0.0197	0.0366	0.0581*
RC10A	<i>0.1365</i>	<i>0.4011</i>	<i>0.3541</i>	<i>0.3287</i>	<i>0.4695</i>	<i>0.3464</i>		0.0457	0.0544*	0.0582*	0.0763*
RC11A	<i>0.2989</i>	<i>0.2938</i>	<i>0.2065</i>	<i>0.1187</i>	<i>0.2487</i>	<i>0.2071</i>	<i>0.2295</i>		-0.0035	0.0259	0.0179
RC11B	<i>0.2696</i>	<i>0.2414</i>	<i>0.1631</i>	<i>0.0766</i>	<i>0.1448</i>	<i>0.1700</i>	<i>0.3007</i>	<i>0.0684</i>		-0.0011	0.0163
RC11C	<i>0.3100</i>	<i>0.2402</i>	<i>0.1157</i>	<i>0.0994</i>	<i>0.2331</i>	<i>0.2323</i>	<i>0.3723</i>	<i>0.2081</i>	<i>0.0589</i>		0.0169
RC11D	<i>0.2225</i>	<i>0.3240</i>	<i>0.1177</i>	<i>0.1145</i>	<i>0.2802</i>	<i>0.2610</i>	<i>0.3815</i>	<i>0.1453</i>	<i>0.1225</i>	<i>0.1156</i>	

Figure S1. Quantification of DNA in *Alexandrium minutum* cultures in comparison with nuclei isolated from human blood cells (HBC, 6.4 Mbp), after staining with propidium iodide in PBS buffer. HBC and *A. minutum* are discriminated on the forward scatter (X-axis, logarithmic scale), a proxy of size, versus red fluorescence (Y-axis, linear scale) dot plot (A). Quantification of DNA (X-axis, linear scale) by fluorescence in two monoclonal strains (B) and (C).

Figure S1:

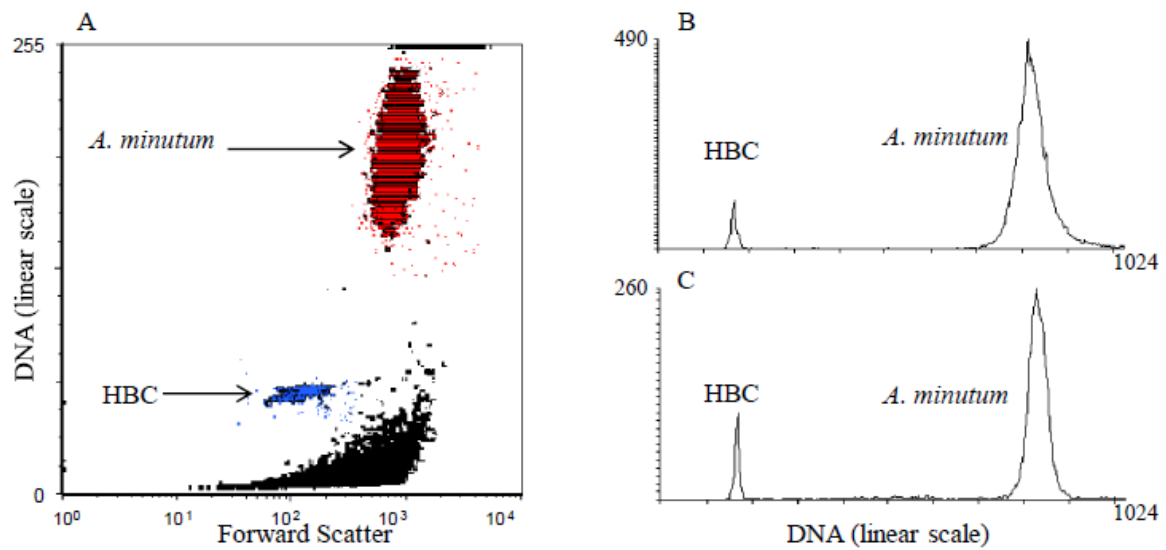


Figure S2. Resolving power of the microsatellite marker set to discriminate the maximum clonal diversity available in the data set.

